Expedited Publications, Original Article

Orbital magnetic resonance imaging profile and clinicoradiological correlation in COVID-19-associated rhino-orbital-cerebral mucormycosis: A single-center study of 270 patients from North India

Maya Hada, Parul Gupta[1], Meenu Bagarhatta[1], Koushik Tripathy[2], Anita Harsh[3], Kamlesh Khilnani, Kuldeep Mendiratta[1], Sunita Agarwal[4], Jugal Kishore Chouhan, Sudhir Bhandari[5]

Purpose: To study the clinical profile and magnetic resonance imaging (MRI) features in patients of COVID-19-associated rhino-orbital-cerebral mucormycosis (CA-ROCM) with orbital involvement and perform a clinicoradiological correlation. **Methods**: A cross-sectional study was performed at a tertiary care center in north India from May 2021 to June 2021. Consecutive patients with clinical, nasal endoscopic, and/or microbiological evidence of CA-ROCM underwent MRI of paranasal sinuses, orbit, and brain as per the study protocol. Orbital MRI findings were studied in detail and were correlated with clinical signs. **Results**: Two hundred and seventy patients were studied. The mean age was 48.4 (± 16.82) years. A male predilection was noted (male:female = 1.77). Orbital involvement was seen in 146 (54%) patients on clinical evaluation and in 184 (68%) patients on MRI. Unilateral orbital involvement was more common (134; 92%). The most common presenting symptom was periorbital and/or facial pain (141; 52.2%) and the most common clinical sign was periorbital edema (116; 43%). The most common MRI finding was suggestive of orbital cellulitis (160; 59%). Orbital compartment syndrome was found in 17 (6.3%) patients. The inter-rater agreement between clinical and radiological assessments to detect the involvement of infraorbital nerve and frontal nerve was found to be 85.56%, (κ 0.621) and 93.70% (κ 0.776), respectively. The diagnostic accuracy, sensitivity, and specificity of MRI to detect medial orbital wall defect were found to be 87.9%, 65%, and 97%, respectively. **Conclusion:** Orbital imaging features of a cohort of ROCM patients have been presented with clinicoradiological correlation.

Key words: COVID-19, MRI, mucormycosis, orbital, ROCM

Access this article online

Website: www.ijo.in

DOI: 10.4103/ijo.IJO_1652_21

Quick Response Code:

India started facing the second wave of COVID-19 pandemic in early 2021. Following the peak of the second wave, a surge of cases of a potentially fatal invasive fungal infection, mucormycosis was encountered across the country, in recovered or active COVID-19 infected patients.[1] COVID-19-associated rhino-orbital-cerebral mucormycosis (CA-ROCM) was declared as an epidemic and/or notifiable disease by many states including Rajasthan, where the study was conducted.

Radiology has a definitive role in the diagnosis and management of CA-ROCM and magnetic resonance imaging (MRI) has been the imaging of choice for the diagnosis as well as to determine the extent of involvement in this condition.[2] Mucormycosis leads to tissue necrosis and MRI provides a superior soft-tissue resolution, a better assessment of devitalized tissues, vascular and perineural invasion, and intracranial involvement, as compared to computed tomogram (CT) scan.[3]

CA-ROCM in its initial stages affects the paranasal sinuses, which is followed by the involvement of the orbit. Orbital spread may occur through the lamina papyracea, nasolacrimal duct, and orbital floor.[4] The presence and extent of orbital involvement affect the clinical presentation, management, and prognosis of CA-ROCM.[5] Therefore, it is of utmost importance for ophthalmologists to understand the MRI features of CA-ROCM for early diagnosis, timely intervention, better surgical planning, and prognostication of these cases.

However, ROCM being a rare occurrence in the pre-COVID-19 era, there is a paucity of major studies to understand the radiological features of this entity. In this study, we aim to demonstrate the MRI features of orbital involvement in CA-ROCM and correlate them with the clinical presentation. We also aim to detect the diagnostic accuracy of MRI in detecting certain clinical parameters in CA-ROCM.

Methods

We performed a cross-sectional study at a tertiary care referral center for CA-ROCM. Institutional review board approval

Departments of Ophthalmology, [1]Radiodiagnosis, [3]Pathology, [4]Otorhinolaryngology and [5]Medicine, SMS Medical College and Hospital, Jaipur, Rajasthan, [2]Department of Ophthalmology, ASG Eye Hospital, Kolkata, West Bengal, India

Correspondence to: Dr. Maya Hada, Assistant Professor, Oculoplastics and Ocular Oncology Services, SMS Medical College and Hospital, Jaipur - 302 004, Rajasthan, India. E-mail: mayahada@gmail.com

Received: 17-Jun-2021 Revision: 22-Aug-2021
Accepted: 25-Nov-2021 Published: 27-Jan-2022

Cite this article as: Hada M, Gupta P, Bagarhatta M, Tripathy K, Harsh A, Khilnani K, *et al*. Orbital magnetic resonance imaging profile and clinicoradiological correlation in COVID-19-associated rhino-orbital-cerebral mucormycosis: A single-center study of 270 patients from North India. Indian J Ophthalmol 2022;70:641-8.

was obtained for the conduct of this study. Consecutive patients of suspected CA-ROCM presenting at our institution from 10th May 2021 to 10th June 2021 underwent a detailed clinical evaluation by a team of otorhinolaryngologists, ophthalmologists, physicians, and neurologists. History regarding the interval between COVID-19 infection to onset of ROCM symptoms, steroid use, diabetic status, and presenting symptoms of ROCM was recorded. Features of ocular or orbital involvement were noted in detail. Optic nerve involvement was diagnosed based on clinical history, best-corrected visual acuity (BCVA), relative afferent pupillary defect, color vision, and fundus examination.

As per the institutional protocol, all patients with clinical suspicion of CA-ROCM were subjected to diagnostic nasal endoscopy, KOH-mount of biopsy samples, culture, and laboratory tests.

Patients with a history of COVID-19 infection or contact with COVID-19 infected person, in association with clinical, nasal endoscopic, and/or microbiological evidence of ROCM were included in the study.

The patients underwent MRI of paranasal sinuses, orbit, and brain as per the protocol mentioned subsequently. Patients on high flow or invasive oxygen support, or with critical systemic status or contraindications for MRI were excluded. Patients in whom MRI and/or any surgical intervention had been performed before the presentation to our institute were also excluded.

All investigations (including MRI) and treatment costs were waived off by the state government in the wake of the exceptional situation of an epidemic. Informed consent was taken from all patients recruited in the study. The study adhered to the tenets of the declaration of Helsinki.

Protocol and sequences of MRI

MRI study was performed in supine position with dedicated head coil on 3T Philips Ingenia MR Scanner (Philips, Eindhoven, Netherlands). An initial T1-weighted (T1W) sagittal scout image was used as a localizer to obtain coronal T1W, T2-weighted (T2W), and T2W fat-suppressed (FS) images; axial T2W FS images and T1W images; and sagittal T2W FS images for the assessment of orbits. Additionally, fluid-attenuated inversion recovery (FLAIR) images were obtained for a complete assessment of the brain along with diffusion-weighted imaging (DWI) in the axial plane and gadolinium (Gd) contrast-enhanced (CE) 3 plane T1W FS images for the assessment of both orbits and brain.

The axial scan was acquired from the top of frontal sinuses superiorly up to the level of the chin inferiorly. The coronal scans were taken from the tip of the nose up to the level of the brainstem. Three-millimeter-thick slices were used with minimal/no interslice gap. Thinner sections of 1.5 mm were obtained in contrast-enhanced scan for better evaluation of the orbital apex, cavernous sinus, cranial nerves, and for vascular assessment. Detailed findings on MRI study of paranasal sinuses, orbit, and brain were noted.

Comments were made on various findings in the orbit including soft tissue and fat strandings in extraconal, intraconal, preseptal spaces; thickening of extraocular muscles (EOMs), optic nerve involvement, abnormal globe signal, globe proptosis or deformity, intraorbital or subperiosteal abscess, orbital apex involvement, perineural involvement of branches of the trigeminal nerve, erosion of orbital walls, involvement of lacrimal sac and nasolacrimal duct; and thrombosis of the superior ophthalmic vein, cavernous sinus, and internal carotid artery. The abnormal globe signal or intensity was seen in cases with associated vitreous hemorrhage/exudates (in panophthalmitis in our series) leading to increased T1W/low T2W signal. Identification of these findings was done by the radiologists based on their characteristic appearance on specific MRI sequences, as follows:

1. The optic nerve involvement on MRI was defined as inflammatory or ischemic. Presumed inflammatory optic nerve involvement was identified as thickening and hyperintensity of the optic nerve, perioptic fat stranding with loss of perioptic CSF (cerebrospinal fluid) sleeve, and contrast enhancement along the optic nerve. Presumed ischemic involvement of optic nerve was considered with the presence of restricted diffusion demonstrated as hyperintensity on DWI images with corresponding low apparent diffusion coefficient (ADC) values [Fig. 1a-e].
2. The thickening and edema of EOMs were evaluated on coronal and axial scans as a high-intensity signal on T2W/T2W FS images and enhancement on gadolinium-based contrast images [Fig. 1d]. Nonenhancement of edematous muscle with low ADC values was interpreted as infarction [Fig. 1f]. Loss of vascularity of the orbital tissues/EOM as evident by loss of contrast enhancement was assessed to determine the extent of devitalized tissue and to plan management.
3. Orbital compartment syndrome was evaluated on axial scans of MRI and was defined as marked fat stranding and thickening of the EOMs, associated with stretching of the optic nerve and distortion or tenting of the globe, resulting in "guitar pick" configuration [Fig. 1e and f]. Optic nerve stretching was recognized when the optic nerve was lying in a straight line between the posterior globe and the orbital apex, with no natural curves on the axial T2W scan.
4. Perineural spread along the branches of cranial nerves was identified as hyperintensity of nerves on T2W image, thickening or enhancement along the nerve course, and infiltration of the fat on T1W images [Fig. 2a-c].
5. Orbital apex involvement was identified as abnormal soft-tissue infiltration and fat stranding in superior and/or inferior orbital fissures on coronal scans [Fig. 2d].
6. Superior ophthalmic vein (SOV) thrombosis was seen as dilation or prominence of SOV and lack of enhancement on gadolinium-based contrast images [Fig. 2d]. Cavernous sinus thrombosis was identified as convex bulging of lateral margin, enlargement of the cavernous sinus with poor contrast enhancement, or filling defects on post-contrast images. Internal carotid artery thrombosis was defined as a lack of contrast opacification due to an intraarterial filling defect on T2W images [Fig. 2e-h].
7. Orbital cellulitis was evaluated with T1W and FS images, as fat stranding in extraconal and intraconal compartments [Fig. 3a]. Preseptal cellulitis was evaluated on axial images as a high signal on T2W FS images.
8. Bone erosions were identified as loss of dark signal from the cortical bone. Assessment of thin bones like lamina papyracea was performed using 1.5 mm slice sequences [Fig. 3a-f]. Asymmetric dural thickening and enhancement was specifically observed and was found

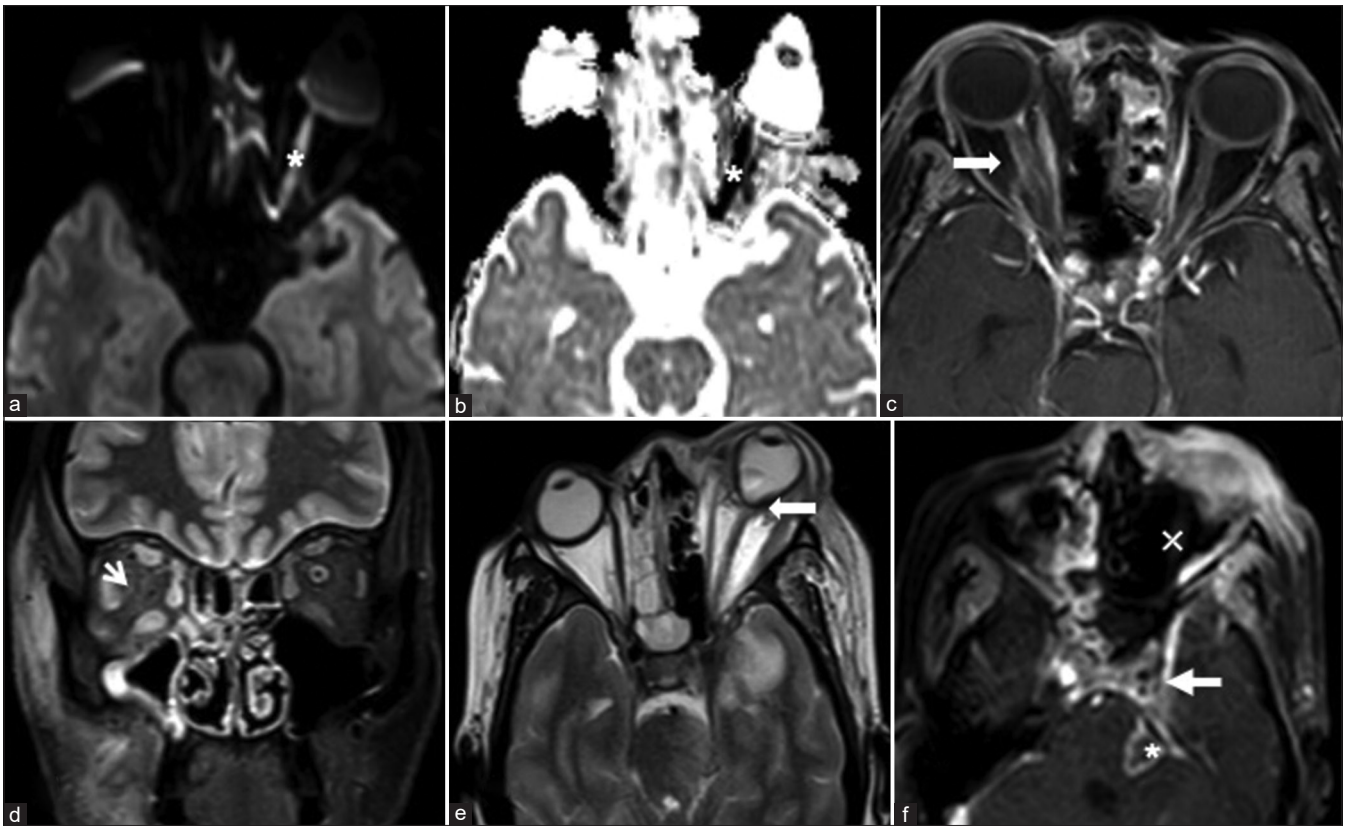

Figure 1: (a and b) DWI (a), and ADC map (b) diffusion restriction* in left optic nerve. (c) CE T1W FS image: enhancement and thickening of the right optic nerve (arrow) and sheath. (d) T2W FS image: fat stranding in right orbit with hyperintense EOMs, loss of perioptic CSF sleeve (arrow) suggesting orbital cellulitis and optic nerve involvement. (e) T2W image: guitar pick sign (arrow). Left medial temporal lobe changes suggest encephalitis secondary to contiguous involvement from the cavernous/paracavernous disease. (f) CE T1W FS image: left orbital infarction (x), left cavernous sinus thrombosis (arrow), abscess formation in left pons*

predominantly in temporal and frontal regions near the areas of bone erosion.

9. An intraorbital abscess was identified as rim enhancement with central hypointensity and diffusion restriction [Fig. 3d-f].
10. Proptosis was detected and measured on axial scans by calculating the distance of the anterior surface of the globe on both sides, from the inter-zygomatic line. A measurement of >23 mm was labeled as proptosis.

MRI findings were correlated with the clinical signs and intraoperative findings. Intraoperative and histopathological findings were noted in patients undergoing surgical intervention and histopathological evaluation.

Statistical analysis

The data analysis was performed using SPSS version 20 [International Business Machines Corporation (IBM), New York, USA] and Microsoft Excel version 16.0 (Microsoft Corporation, Washington, USA). A *P* value of ≤0.05 was considered significant. Correlation coefficient κ was used to measure the extent of agreement between various clinical and radiological variables. The κ values range from −1 to 1, with 1 presenting complete agreement and 0 meaning no agreement or independence.

Results

Three hundred and forty-two patients of CA-ROCM were clinically evaluated in the study period. Twenty-five patients with critical systemic status, 4 patients with contraindications for MRI, and 33 patients, in whom MRI was performed before the presentation to our institute, were excluded. Ten patients with no history of COVID-19 infection or contact with COVID-19 infected persons were excluded.

Two hundred and seventy patients were studied. The demographic, clinical, and radiological findings of the patients are listed in Table 1. The mean age of presentation was 48.4 ± 16.82 (median 52, range 20–82) years. There were 173 males (M) and 97 females (F) (M:F = 1.77). The mean duration between the COVID-19 infection and onset of CA-ROCM was 12.4 (median 11, range 4–34) days. History of steroids use was present in 195 (72%) patients (mean duration of steroid use = 6.4 days). A history of diabetes mellitus was present in 249 (92.2%) patients.

Orbital involvement was seen in 146 (54%) patients on clinical evaluation. Unilateral orbital involvement was seen in 134 (92%) and bilateral involvement was seen in 12 (8%) patients. The most common presenting symptoms were periorbital and/or facial pain (n = 141) followed by facial swelling (n = 125) and numbness (n = 103). The most common clinical sign was periorbital edema (n = 116). Vision loss (BCVA ≤ 20/200) was present in 28% (n = 76) of patients, ophthalmoplegia was noted in 31.6% (n = 86), and proptosis was detected in 18% (n = 49) of patients on examination. However, these signs were perceived as primary symptoms only in 9% (dimness of vision noticed

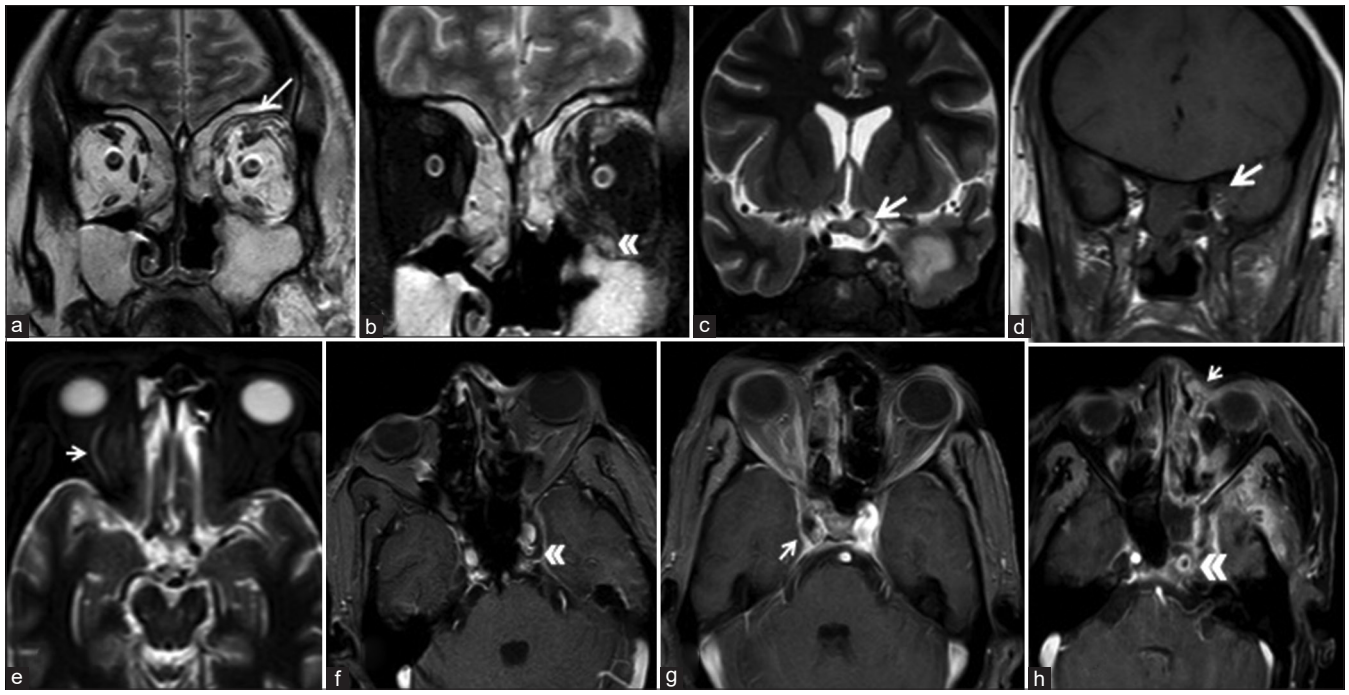

Figure 2: (a-c) T2W (a) and T2W FS images (b and c): thickening of left frontal (arrow in a), infraorbital nerve (double arrowhead in b), and optic chiasma (arrow in c). (d) T1W image: loss of normal fat signal along left superior and inferior orbital fissure (arrow). (e) T2W FS image: prominent right superior ophthalmic vein (arrow) with loss of normal signal flow void. (f-h) CE T1W FS image: convexity and nonenhancement of the left cavernous sinus (double arrowhead in f), filling defect in the right internal carotid artery (arrow in g), suggesting thrombosis. Left lacrimal sac hyperintensity (arrow in h) and nonenhancement of the left cavernous sinus (double arrowhead in h) are also needed

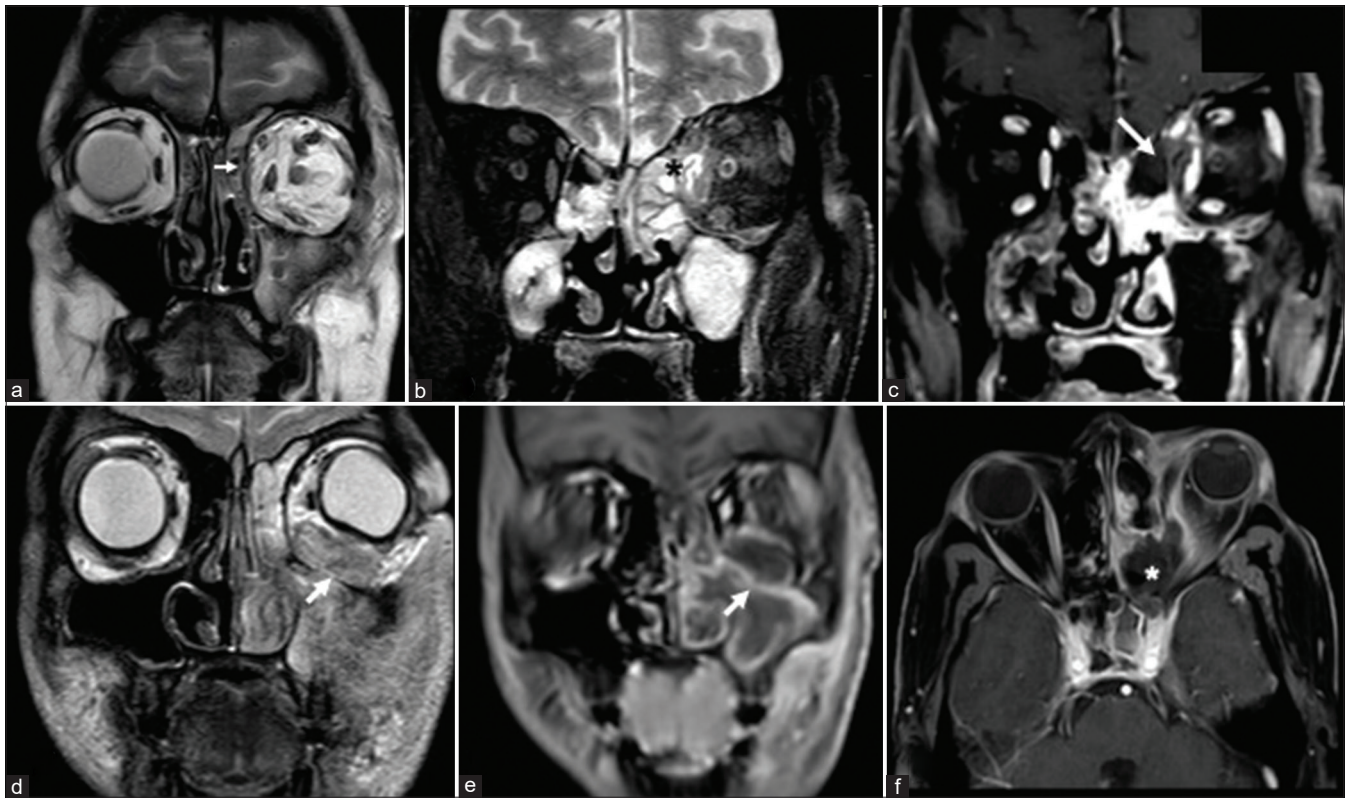

Figure 3: (a-c) T2W (a), T2W FS (b), and CE T1W FS image (c) showing a loss of normal signal of the cortical bone in the medial wall of the left orbit: a defect in left lamina papyracea (arrow in a), hyperintensity in the ethmoid sinus (* in b), and nonenhancing collection (arrow in c) extending in medial extraconal space through the defect. d-e. T2W (d) and CE T1W FS image (e) showing left maxillary sinusitis with the breach in the left orbital floor (arrow in d), rim enhancing collection, and restricted diffusion (not shown), suggesting abscess (arrow in e). (f) T1W FS CE image showing nonenhancing contents in the left ethmoidal sinus, extending in medial orbit through the defect in the medial wall*

Table 1: Demographic, clinical, and orbital MRI features of 270 patients of CA-ROCM

Features	No. of patients (270)
Age	
Mean, years	48.4
Median (range), years	52 (20-82)
Gender	
Male	173 (64%)
Female	97 (36%)
Primary symptoms	
Periorbital/facial pain	141 (52.2%)
Periorbital/facial swelling	125 (46.29%)
Numbness/paresthesia	103 (38.14%)
Ptosis	44 (16.3%)
Ocular movements limitation	38 (14%)
Diminished or loss of vision	25 (9.25%)
Nasal blockade/discharge	24 (8.8%)
Discoloration of periorbital/facial skin	18 (6.6%)
Palatal ulcer/eschar	10 (4%)
forward bulging of the eye	8 (3%)
Orbital/Ophthalmological signs	
Periorbital edema/cellulitis	116 (43%)
Ophthalmoplegia	86 (31.6%)
Total	68 (25%)
Partial	18 (6.6%)
Ptosis	79 (29%)
Total	68 (25%)
Partial	11 (4%)
Vision loss	76 (28%)
No PL	52 (19%)
≤20/200 to PL	24 (8.8%)
CRAO	26 (9.6%)
Periorbital hypaesthesia	
Infraorbital	82 (30%)
Frontal	51 (18.8%)
Proptosis	49 (18%)
Panophthalmitis	26 (9.6%)
Globe deformity	12 (4.4%)
Globe perforation	5 (1.8%)
Eyelid eschar/necrosis	6 (2%)
Orbital MRI findings	
Orbital and Preseptal cellulitis	160 (59.25%)
Intraconal fat stranding	125 (46.29%)
Extraconal fat stranding	114 (42.2%)
Preseptal fat stranding	146 (54%)
Intraorbital Abscess	22 (8.14%)
Orbital Compartment syndrome	17 (6.3%)
Extraocular muscle involvement	127 (47%)
MR	119 (44%)
IR	108 (40%)
LR	97 (36%)
SR/LPS	78 (29%)
Optic Nerve involvement	52 (19.2%)
Optic nerve thickening	47 (17%)
Loss of perioptic sleeve of CSF	43 (15.9%)
DWI restriction/ischemic optic neuropathy	36 (13.3%)
Optic nerve stretching	17 (6.3%)
Orbital apex involvement	25 (9.25%)
Superior orbital fissure	25 (9.25%)
Inferior orbital fissure	22 (8.14%)
SOV thrombosis	27 (10%)
Cavernous Sinus Thrombosis	22 (8.14%)
ICA thrombosis	17 (6.3%)
Globe proptosis	77 (28%)
Abnormal globe signal intensity	30 (11%)
Globe deformity/tenting	14 (5.18%)
Dehiscence of uveoscleral coat	6 (2.2%)
Perineural invasion	
Infra-orbital nerve involvement	65 (24%)
Frontal nerve involvement	38 (14%)
Lacrimal Sac/Nasolacrimal duct involvement	77 (28%)
Bone erosions	
Medial wall erosion	70 (26%)
Inferior wall erosion	38 (14%)
Superior wall erosion	11 (4%)

PL: perception of light; MR: medial rectus, LR: lateral rectus; IR: inferior rectus; SR/LPS: superior rectus/levator palpebrae superioris; CSF: cerebrospinal fluid; DWI: diffusion-weighted imaging; SOV: superior ophthalmic vein; ICA: internal carotid artery

by the patient), 14% (limited ocular movements), and 3% (forward bulging of the eye) of patients. In patients with bilateral involvement, the primarily affected eye was diagnosed to have total ophthalmoplegia with vision loss in 10 cases, and panophthalmitis and globe deformation in one case each. In the other eye, ophthalmoplegia with vision loss was present in 9 patients, ophthalmoplegia was noted in 2 cases, and preseptal cellulitis was seen in 1 case.

Sixty-eight percent of patients (n = 184) showed orbital involvement on MRI. The most common finding on MRI was suggestive of orbital and preseptal cellulitis (n = 160; 59%). The preseptal fat stranding was present in 54% of patients, which correlated with the most common clinical sign of periorbital edema in 43% of patients. EOM thickening was seen in 47% of patients and the medial rectus was the most common muscle to be involved (n = 119; 44%) in MRI. Optic nerve involvement in MRI was seen in 52 (19.2%) patients. Of these, presumed inflammatory thickening of the optic nerve was most common (n = 47; 17%) followed by presumed ischemic involvement of the optic nerve (n = 36; 13.3%). Optic nerve stretching was seen in association with orbital compartment syndrome in 17 (6.3%) patients.

All 17 patients with orbital compartment syndrome demonstrated significant resistance to retropulsion on clinical evaluation (P-value < 0.05) and 11 (4%) cases demonstrated loss of contrast enhancement in EOMs and optic nerve. Of these, 4 patients also showed infarction of ethmoidal sinuses and avascular necrosis of adjacent bones, forming a larger phlegmonous area. In these patients, eyelid edema (9), eschar over medial canthus and eyelids (4), and ulceration and necrosis of medial canthus and eyelids (2) were clinically seen. The association with the presence of eyelid eschar and necrosis on clinical examination was statistically significant (P-value <0.05).

Involvement of the apex of the orbit on MRI was seen in 25 (9%) patients. All these patients had no perception of light (no PL) and ophthalmoplegia on clinical evaluation. Causes of vision loss in cases of ROCM include central retinal

arterial or ophthalmic artery occlusion, involvement of the optic nerve (invasion, ischemic, inflammatory, or tractional), increased intraocular pressure, exposure keratopathy, media haze, and involvement of the vitreous and ocular coats.[6]

Cases with corneal melt, panophthalmitis, and deformed globe were carefully examined. Those with radiological evidence of optic nerve stretching, ischemia, inflammation, and invasion were also included in optic neuropathy-related vision loss. These patients had history of vision loss before the development of keratopathy, globe deformity, and panophthalmitis. Poor visual outcome was most commonly associated with optic nerve involvement.

Features suggestive of the superior ophthalmic vein, cavernous sinus, and internal carotid artery thrombosis were seen on MRI in 27 (10%), 22 (8.14%), and 17 (6.3%) patients, respectively. All these patients demonstrated significant association with the presence of ophthalmoplegia on clinical evaluation (P-value < 0.05).

On MRI, proptosis of the eyeball was noted in 28% of patients, while on clinical examination, proptosis was detected in only 18% of patients (mean 3.12 ± 1.2 mm) (P-value >0.05). Abnormal globe intensity, globe deformity, and dehiscence (discontinuity) of uveoscleral coat were noted with MRI in 30 (11%), 14 (5%), and 6 (2.2%) patients, respectively, which correlated significantly with the clinical findings of panophthalmitis, deformed globe, and globe perforation in 26 (9.6%), 12 (4.4%), and 5 (1.8%) patients, respectively.

We categorized our patients as per the ROCM staging system proposed by Honavar.[5] Out of the 184 patients with radiological signs of orbital involvement, 24 (13%) patients were in stage 3a, 72 (39%) cases were in stage 3b, 76 (41.3%) patients were in stage 3c, and 12 (6.5%) cases were classified as stage 3d. Fifty-four patients had intracranial involvement, and pachymeningitis was the most common intracranial finding, which was seen in 42 patients.

We also assessed certain parameters like perineural invasion along infraorbital and frontal nerves clinically, and erosion of lamina papyracea based on intraoperative findings and correlated with MRI findings. Clinically the presence of perineural invasion was determined by the presence of hypoesthesia in the areas innervated by infraorbital and frontal nerves, whereas breach in lamina papyracea was confirmed intraoperatively as defect or erosion in the medial orbital wall.

Out of 270 patients, based on clinical assessment, 82 (30%) and 51 (18.8%) patients showed involvement of infraorbital and frontal nerve, respectively, whereas MRI detected thickening or infiltration of the infraorbital nerve in 48 (17.7%) and frontal nerve in 37 (13.7%) patients. The inter-rater agreement between clinical and radiological assessments to detect the involvement of infraorbital nerve was 85.56%, (κ 0.621 ± 0.053; C. I. 0.516 to 0.725) and that of the frontal nerve was 93.70% (κ 0.776 ± 0.052; C. I. 0.675 to 0.877).

Out of the 215 patients, who underwent endoscopic sinus surgery, a breach in lamina papyracea was noted intraoperatively in 80 (37.2%) patients, whereas MRI showed medial wall defect in 58 (26.9%) patients. The diagnostic accuracy, sensitivity, and specificity were found to be 87.9%, 65%, and 97%, respectively.

Of the 17 patients having diffuse orbital involvement, 9 underwent orbital exenteration surgery during the study period.

Angioinvasion was seen on histopathology in 7 (77%) patients. The fungal hyphae were identified in the wall as well as in the lumen of blood vessels forming thrombi with adjacent tissue necrosis on histopathology [Fig. 4a]. Granulomatous inflammation was noted in 6 (66%) patients. The fungal hyphae were identified infiltrating the intraorbital fat with areas of necrosis [Fig. 4b]. Perineural invasion was seen histopathologically in 5 (55%) cases.

Neutrophilic and lymphocytic infiltration was mild in 3 cases [Fig. 4c] and moderate to marked in 6 cases. Necrosis of ocular coats was evident in histopathology in 3 (33%) cases [Fig. 4d].

Discussion

The purpose of this study was to characterize the whole spectrum of abnormal orbital findings on MRI in patients with CA-ROCM and to correlate those abnormalities with clinical features or intraoperative findings.

The mean age of presentation in our study was 48.4 years and there was a male predilection (64%) noted, which was consistent with the existing epidemiological data on CA-ROCM.[7,8] The use of systemic steroids has been implicated in the etiopathogenesis of COVID-19 associated mucormycosis.[9] In our study, 72% of patients had a history

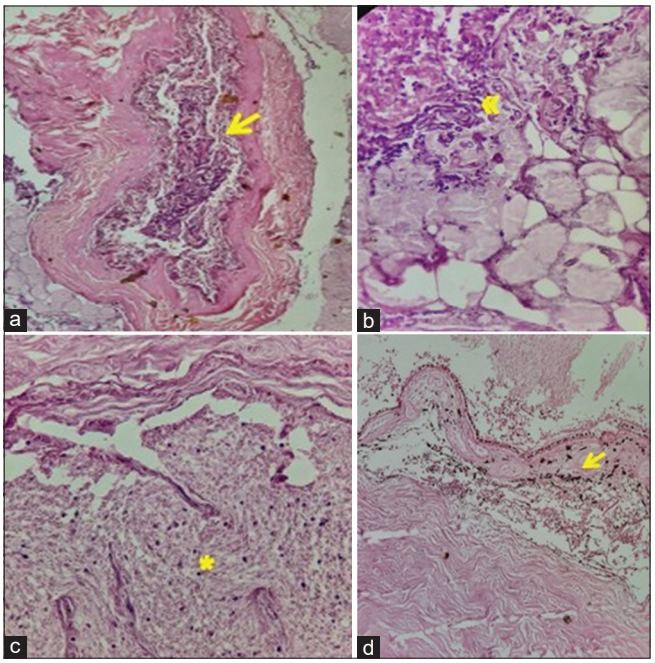

Figure 4: (a) Photomicrograph showing angioinvasion; lumen of the blood vessel obliterated by a mycotic thrombus (arrow) (H and E, ×10). (b) Photomicrograph showing orbital fat infiltration by aseptate hyphae (double arrowhead) (H and E, ×10). (c) Photomicrograph of a cut section of optic nerve showing vacuolar degeneration and lymphocytic infiltration (*) (H and E, ×40). (d) Photomicrograph showing degenerative and necrotic changes in the sclera (arrow) and choroid (H and E, ×10)

of systemic steroids intake. Diabetes mellitus is known to be the single most important risk factor for mucormycosis.[10,11] In our series also, 92.2% of patients were having diabetes before the onset of CA-ROCM. COVID-19 associated ROCM has been reported to occur in patients with active as well as in recovered COVID-19illness.[12] In our study, the majority of patients developed CA-ROCM at the end of the second-week post-COVID-19 infection (mean interval 12.4 days).

In our study, the signs of orbital involvement on MRI were present in 68% of patients as compared to 54% of patients having clinical signs of orbital disease. This may indicate that the radiological signs can detect the disease before it is clinically apparent. In two retrospective studies of 23 and 43 patients of acute invasive fungal rhinosinusitis, orbital involvement on imaging was noted in 65% and 76%, respectively, which was consistent with our series.[13,14]

In all cases of our series, the sequential involvement of nose-sinus-orbit-CNS (central nervous system) was there, although there were cases of intracranial abscesses with noncontiguous involvement. Also, the disease progressed to CNS without complete/diffuse involvement of the orbit in the majority of cases, signifying that stage 4 disease may occur without stage 3c or 3d.

In our study, a significant association was noted between the presence of orbital compartment syndrome on MRI and positive retropulsion test on clinical examination. This radiological finding with supportive evidence of clinical examination suggests increased intraorbital pressure within the closed compartment of the orbit and warrants early surgical intervention. The orbital compartmental syndrome has been reported in CA-ROCM.[15] In our study, 17 (6.3%) patients had clinical and radiological evidence of this condition, of which 9 underwent orbital exenteration during the study period. Thus, the management of CA-ROCM patients was largely based on radiological findings. Patients with diffuse orbital involvement and/or orbital compartment syndrome as suggested by optic nerve stretching and globe tenting were managed with exenteration. Cases with limited orbital involvement (extraconal/without signs of optic nerve stretching or globe tenting) were treated with endoscopic clearance/debridement with globe salvage. The patients with or without vision loss, with signs of orbital involvement, not amounting to exenteration were treated with transcutaneous retrobulbar amphotericin B (TRAMB).

In our experience, 3% (n = 9) overall mortality was found during the study period. All patients had intracranial involvement. No mortality was found in cases where the disease was limited to orbit in our series. In our experience beyond the study period, increased mortality was associated with poor systemic status as well as multiple brain abscesses. In a large review of 929 reported zygomycosis cases,[16] the mortality rate was 54%. The highest risk of mortality was associated with disseminated disease, infection of the lung, sinuses, brain, kidney, and gastrointestinal tract.[16] The study noted that the rate of mortality in sinus disease overall was 46%.[16] The mortality rates of various sites of infection were 87% in sinopulmonary disease, 62% in rhinocerebral disease, 24% in sino-orbital infection, and 16% in isolated sinusitis.[16] Yohai and colleagues[17] showed that lower survival was associated with late diagnosis and management, bilateral sinus disease, hemiplegia or hemiparesis, kidney disease, leukemia, and treatment with deferoxamine.

The presence of orbital apex involvement and/or thrombosis of the superior ophthalmic vein, cavernous sinus, and internal carotid artery on MRI was found to have a significant association with the presence of ophthalmoplegia, indicating a multifactorial etiology of ophthalmoplegia in these cases.

Restricted diffusion in the path of mucor invasion was demonstrated on DWI sequences in 36 (13.3%) patients. This phenomenon is related to the ischemia and necrosis resulting from the angioinvasive nature of mucormycosis.[18]

Presence of globe contour abnormalities, dehiscence of ocular coats, and inflammation of the coats of the eyeball on MRI significantly correlated with corresponding clinical findings, suggesting MRI as a reliable tool for detecting globe abnormalities radiologically.

Perineural invasion was found to be an early feature of mucormycosis as evident by the presence of numbness and paresthesia as a primary symptom in 38% of patients in our series. Most commonly the branches of the trigeminal nerve were affected, which were identified on MRI by thickening and enhancement along the course of the nerve. In our study, MRI was found to be a sensitive tool to detect the involvement of infraorbital and frontal nerves, which corresponded well with clinical assessment (85.5% and 93.7%, respectively).

The medial wall of the orbit acts as a barrier between the ethmoid sinus and orbit. Breach in the medial wall is an important early sign of orbital invasion by mucormycosis. In our study, MRI showed 65% sensitivity, 88% accuracy, and high specificity (97%) in detecting erosion of lamina papyracea. We suggest that careful evaluation on MRI can help in detecting subtle bony erosions and second imaging (CT scan) may be avoided to look for the same.

We found the histopathological findings of angioinvasion (77%), perineural invasion (33%), tissue necrosis (55%), and granulomatous inflammation (66%) in exenterated specimens of CA-ROCM. Similar pathological changes on biopsy samples were noted in a few retrospective studies.[19,20] Further studies are needed to correlate histopathological and radiological findings, with a larger sample of exenterated specimens.

We re-emphasize that the interpretation of orbital features on MRI is critical for assessing the extent of involvement and planning of appropriate management. In the presence of MRI features of cellulitis without signs of ischemia, as demonstrated by contrast enhancement of orbital soft tissues on MRI, medical management remains the mainstay of management for orbital disease.[21] Whereas, if the ischemic necrosis/infarction of the orbital tissues is evident, as demonstrated by diffusion restriction and nonenhancement of the soft tissues, surgical debridement of the devitalized tissue is required. The decision for orbital exenteration is substantially dependent on the radiological evidence of diffuse orbital involvement and features of orbital compartment syndrome, which can be best evaluated on MRI.[22]

Conclusion

Orbital MRI features correlated well with the clinical features in our cohort of patients of ROCM and MRI was found to be a highly valuable tool to diagnose and determine the extent of ROCM in our series. We believe that this clinicoradiological study will improve the understanding of the orbital ROCM and thus help in clinical decision making and patient management.

Financial support and sponsorship

Nil.

Conflicts of interest

There are no conflicts of interest.

References

1. Sen M, Lahane S, Lahane TP, Parekh R, Honavar SG. Mucor in a viral land: A tale of two pathogens. Indian J Ophthalmol 2021;69:244-52.
2. Kaushik KS, Ananthasivan R, Acharya UV, Rawat S, Patil UD, Shankar B, *et al*. Spectrum of intracranial complications of rhino-orbito-cerebral mucormycosis-resurgence in the era of COVID-19 pandemic: A pictorial essay. Emerg Radiol 2021;28:1097-106.
3. Terk MR, Underwood DJ, Zee C-S, Colletti PM. MR imaging in rhinocerebral and intracranial mucormycosis with CT and pathologic correlation. Magn Reson Imaging 1992;10:81–7.
4. Herrera DA, Dublin AB, Ormsby EL, Aminpour S, Howell LP. Imaging findings of rhinocerebral mucormycosis. Skull Base 2009;19:117–25.
5. Honavar SG. Code mucor: Guidelines for the diagnosis, staging and management of rhino-orbito-cerebral mucormycosis in the setting of COVID-19. Indian J Ophthalmol 2021;69:1361–5.
6. Sreshta K, Dave TV, Varma DR, Nair AG, Bothra N, Naik MN, *et al*. Magnetic resonance imaging in rhino-orbital-cerebral mucormycosis. Indian J Ophthalmol 2021;69:1915–27.
7. Garg D, Muthu V, Sehgal IS. Coronavirus Disease (Covid-19) associated mucormycosis (CAM): Case Report and Systematic Review of Literature. Mycopathologia 2021;186:289–98.
8. Singh AK, Singh R, Joshi SR, Mishra A. Mucormycosis in COVID-19: A systematic review of cases reported worldwide and in India. Diabetes Metab Syndr Clin Res Rev 2021;15:102146.
9. Lionakis MS, Kontoyiannis DP. Glucocorticoids and invasive fungal infections. Lancet 2003;362:1828–38.
10. Jeong W, Keighley C, Wolfe R, Lee WL, Slavin MA, Kong DC, *et al*. The epidemiology and clinical manifestations of mucormycosis: A systematic review and meta-analysis of case reports. Clin Microbiol Infect 2019;25:26–34.
11. Patel A, Kaur H, Xess I, Michael JS, Savio J, Rudramurthy S. A multicentre observational study on the epidemiology, risk factors, management and outcomes of mucormycosis in India. Clin Microbiol Infect 2020;26:944.e9-15. doi: 10.1016/j.cmi.2019.11.021.
12. Hoenigl M, Seidel D, Carvalho A, Rudramurthy SM, Arastehfar A, Gangneux JP, *et al*. The Emergence of COVID-19 associated mucormycosis: analysis of cases from 18 countries. Available at:https://papers. ssrn.com/sol3/papers.cfm?abstractid=3844587. [Last accessed on 2021 Jun 15].
13. Choi YR, Kim JH, Min HS, Won JK, Kim HJ, Yoo RE. Acute invasive fungal rhinosinusitis: MR imaging features and their impact on prognosis. Neuroradiology 2018;60:715–23.
14. Therakathu J, Prabhu S, Irodi A, Sudhakar SV, Yadav VK. Imaging features of rhinocerebral mucormycosis: A study of 43 patients. Egypt J Radiol Nucl Med 2018;49:447–52.
15. Werthman-Ehrenreich A. Mucormycosis with orbital compartment syndrome in a patient with COVID-19. Am J Emerg Med 2021;42:264.e5-8. doi: 10.1016/j.ajem. 2020.09.032.
16. Roden MM, Zaoutis TE, Buchanan WL, Knudsen TA, Sarkisova TA, Schaufele RL, *et al*. Epidemiology and outcome of zygomycosis: A review of 929 reported cases. Clin Infect Dis 2005;41:634–53.
17. Yohai RA, Bullock JD, Aziz AA, Markert RJ. Survival factors in rhino-orbital-cerebral mucormycosis. Surv Ophthalmol 1994;39:3–22.
18. Hatipoglu HG, Gurbuz MO, Yuksel E. Restricted diffusion in the optic nerve and retina demonstrated by MRI in rhino-orbital mucormycosis. J Neuroophthalmol 2009;29:13–5.
19. Goel A, Kini U, Shetty S. Role of histopathology as an aid to prognosis in rhino-orbito-cerebral zygomycosis. Indian J Pathol Microbiol 2010;53:253–7.
20. Sravani T, Uppin SG, Uppin MS, Sundaram C. Rhinocerebral mucormycosis: Pathology revisited with emphasis on perineural spread. Neurol India 2014;62:383–6.
21. Pelton RW, Peterson EA, Patel BC, Davis K. Successful treatment of rhino-orbital mucormycosis without exenteration: The use of multiple treatment modalities. Ophthalmic Plast Reconstr Surg 2001;17:62–6.
22. Hargrove RN, Wesley RE, Klippenstein KA, Fleming JC, Haik BG. Indications for orbital exenteration in mucormycosis. Ophthalmic Plast Reconstr Surg 2006;22:286–91.